Evolutionary Generation of 3-D Line-Segment Circuits With a Broadside-Coupled Multiconductor Transmission-Line Model

Tamotsu Nishino, *Member, IEEE,* and Tatsuo Itoh, *Fellow, IEEE*

***Abstract*—Evolutionary generation of three-dimensional microwave line-segment circuits embedded in a multilayer structure is presented. Connections of the line segments and their lengths are expressed by sets of parameters, which are evolutionarily optimized by the genetic algorithms. Practical optimization time is achieved by introducing models of broadside-coupled multiconductor transmission lines instead of full-wave electromagnetic (EM) calculations. The scattering parameters of the models are connected with the scattering parameters of vias, and are synthesized into that of the whole circuit. Using line segments, we can obtain not only small components for limited-space applications, but also large components for wide-band frequency specifications without increasing computational complexity. Two bandpass filters and a bandstop filter were designed and tested by an EM simulator. The bandpass filters were also fabricated and measured. The results validated our proposing procedure.**

***Index Terms*—Filters, genetic algorithms (GAs), line segment, low-temperature co-fired ceramic (LTCC), optimization, three-dimensional (3-D), topology.**

I. Introduction

OPTIMIZATIONS of microwave circuits, especially of filters, have typically been carried out for lengths and/or widths of their lines by conventional methods such as the quasi-Newton method, conjugate gradient method, or random-search technique. Their initial values are obtained from conventional lumped-element prototype circuits.

On the other hand, recent microwave systems require very compact circuits or very eccentric specifications, which are difficult to be obtained by such conventional ways. To design such compact circuits, we need to search solutions not only in the prototype ladder lumped-element circuits, but also in ways of connecting elements in two or three dimensions.

For such purposes, we already have introduced the evolutionary design of two-dimensional (2-D) microwave line-segment circuits by the genetic algorithms (GAs) [1]. In the paper, we applied the GA to microwave circuits to optimize the circuits' topology and lengths. Unlike optimizations with an electromagnetic (EM)-based patch-segment simulation, our approach with line segments did not require a large number of parameters for large circuits. This enabled us to obtain not only narrow-band specifications for small components, but also wide-band specifications for larger ones.

The GA was introduced by Holland in 1975 [2] as a subject of computer science. Recently, it began to be applied to optimizations of discrete and/or discontinuous microwave problems. Michielssen *et al.* applied the GA to optimizations of multilayer structures such as frequency-selective surfaces in 1993 [3]. Johnson and Rahmat-Samii optimized antenna patterns along with the method of moments (MoM) [4]. They reduced computation time by replacing some elements in impedance matrices obtained by the MoM with zeros according to an antenna shape instead of calculating the whole impedance matrices each time. For analog circuits' design, Koza *et al.* synthesized linear and nonlinear circuits, combining the genetic programming with SPICE [5]. As for microwave circuit applications, John and Jansen have developed an excellent way to design (monolithic) microwave integrated circuit (M)MIC components by the GA combined with the two-and-one-half-dimensional (2.5-D) spectral-domain approach (SDA) [6]. This was good for small-size components, but not efficient for large components because of its huge time consumption of EM-based calculations.

In this paper, we devised an expression of three-dimensional (3-D) circuits by a set of parameters, which is optimized by the GA. The expression is derived from our previous 2-D work.

To reduce the computation time, a circuit is decomposed into via models and broadside-coupled multiconductor transmission-line models. There is a huge amount of research on two-conductor transmission-line models and their applications. As for three-conductor models, several great investigations have been done. Pavlidis and Hartnagel have derived side-coupled three-conductor transmission-line models with modal representations of lines [7]. Yamamoto *et al.* have investigated not only side-coupled models, but have also derived a broadside-coupled three-line model [8]. Several books have been published on multiconductor transmission-line models. Paul investigated the models from a point-of-view of transmission-line differential equations, which are described by per-unit-length capacitance, inductance, and resistance matrices [9]. Fache *et al.* have published an excellent work [10], in which they discussed the condition to match EM and circuitry representations. This concept was highly suggestive for our study.

In Section III-C, we extract the capacitance matrix of an m-conductor transmission line of unit length using the 2-D finite-element method (FEM). The procedure is described as a suitable way to be embedded in computer-aided design (CAD)

Manuscript received March 28, 2003; revised April 16, 2003.

T. Nishino is with the Mitsubishi Electric Corporation, Kanagawa 247-8501, Japan (e-mail: nishino@isl.melco.co.jp).

T. Itoh is with the Department of Electrical Engineering, University of California at Los Angeles, Los Angeles, CA 90095 USA.

Digital Object Identifier 10.1109/TMTT.2003.817468

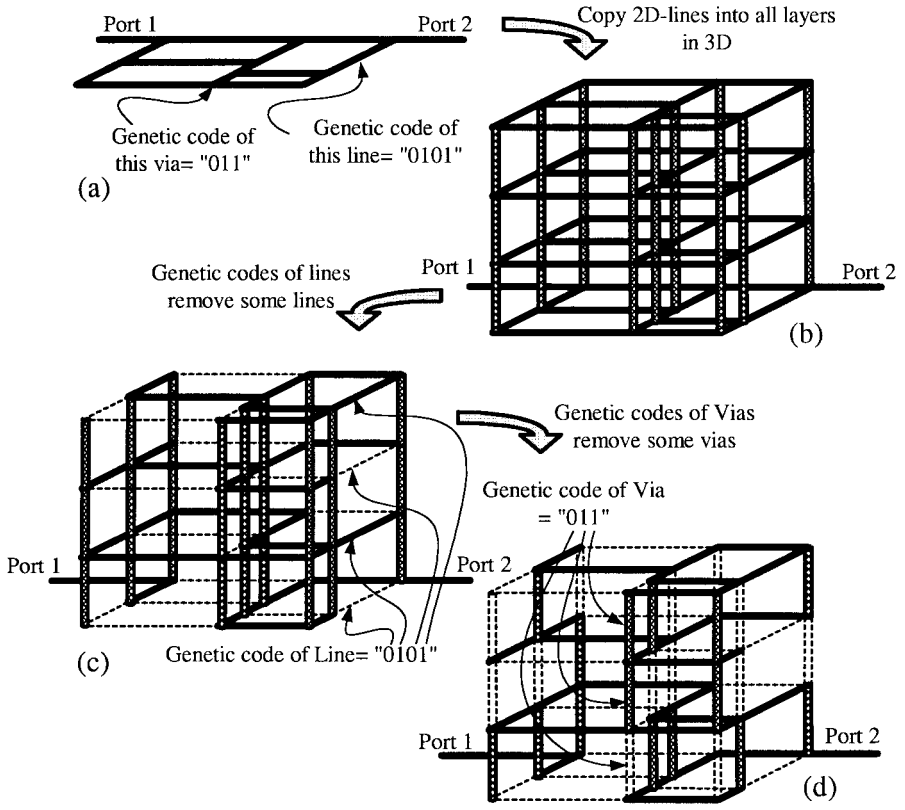

Fig. 1. Process growing 3-D circuits in the case of a four-layer structure. (a) Creation of 2-D P-circuit pattern. (b) Copy of the P-circuit pattern to all layers. (c) Removal of lines corresponding to "0." (d) Removal of vias corresponding to "0."

programs. m intrinsic transmission modes are then obtained. The impedance value of each mode is calculated using the 2-D FEM by exciting m conductors with appropriate voltages, which are not only proportional to the mode voltages, but are normalized to satisfy a condition to equate energy consumptions between EM and circuit representations. The obtained mode impedances are stored in a lookup table, and used to calculate scattering parameters (S-parameters) of m-conductor transmission line of arbitrary length in the GA process. The S-parameters are synthesized with the S-parameters of vias that are precalculated by the MoM. The circuit responses are so calculated that the computation time for one circuit at one frequency is less than 1 s.

The advantages against conventional design procedures are as follows.

- No initial condition is required.
- Multipassbands and/or multistopbands can be specified.
- Not only the one-dimensional ladder-circuit-type properties, but also the multipass network, which realize phase interference effects such as rat-race hybrids, can possibly be proposed to reduce insertion loss due to the Q factor of the resonators.
- Applications to multilayer structures can propose very compact-size circuits that no conventional technique can propose via a straightforward way.

Two bandpass filters and a bandstop filter were designed and tested by an EM simulator. The bandpass filters were also fabricated and measured. The result shows the validity of our proposed models and effectiveness of design by the GA.

II. Genetic Expressions of Growing 3-D Circuits

In [1], a 2-D circuit was expressed by a set of parameters. The parameters described structural growth of the circuit by indicating how new lines would be added successively to an outermost frame circuit, which we called a "base circuit." The line-adding process chose two adjacent parallel lines in the circuit. A new line was then disposed to bridge the two lines perpendicularly. After iteration of this process, some lines were eventually removed from the circuit.

We extended this procedure to 3-D circuits composed in a multilayer structure. Fig. 1 shows this process in the case of a four-layer structure.

First, our GA process generates a 2-D circuit pattern as described in our previous work, except that no line is removed. Let us call this circuit pattern a 2-D projected circuit (P-circuit) pattern. The process also assigns a specific genetic code to each line and to each intersection point [see Fig. 1(a)]. The specific genetic code of a line is an N-bit binary number, where N is the number of layers, and the specific genetic code of an intersection point is an $(N-1)$-bit binary number.

The P-circuit pattern is then copied to all layers in the multilayer structure [see Fig. 1(b)]. The process uses the specific codes described above to determine the existence of lines that were copied from the same line of the P-circuit pattern.

Fig. 1(c) shows the lines whose corresponding line in the P-circuit have a genetic code "0101" remain in layer 2 and 4, and are removed in layer 1 and 3. In this case, for example, the first "0" corresponds to the removal of a line in the first layer (the bottommost one), and the last "1" corresponds to the existence of a line in the fourth layer (the topmost one).

Fig. 1(d) shows the vias whose corresponding intersection point in P-circuit has a genetic code "011." These vias lie between the second and third layer and between the third and fourth layer. In this example, the "0" corresponds to removal of a via between corresponding layers and the "1" corresponds to existence of a via there.

These specific genetic codes representing existence of lines and vias are optimized by the GA, as well as the genetic codes representing the P-circuit's topology and dimensions. We do not mention the GA in this paper. The procedures are the same as what we have proposed in [1].

III. Modeling of a 3-D Line-Segment Circuit

The GA requires models to calculate a circuit's responses quickly since it tests more than tens of thousands circuits before convergence. In this section, models of vias and models of line segments are described.

A. Models of Elements in a Multilayer Structure

Quick calculations of the responses of a circuit are performed by decomposing the circuit into vias and coupled line segments. Synthesizing S-parameters of the decomposed elements to S-parameters of the original 3-D circuit is much faster than the EM-based S-parameter extraction.

Coupling effects between the lines overlapped in different layers are taken into account, while the ones between the lines in the same layer are ignored. This approximation is valid under the condition that two adjacent lines in the P-circuit are disposed with a interval more than a certain minimum value. This condition is also indispensable to avoid generations of closely disposed T-junctions whose interval is less than the line width.

B. Models of Vias

A lookup table made by EM simulations is used for vias since the number of combinations to connect layers through vias is not large. Intersection points in a P-circuit pattern have three types of discontinuities. They are a T-junction, a right-angle corner, and a single end. In an N-layer structure, each intersection point has 2^{N-1} combinations of via connections. Fig. 2 shows four combinations of via connections in a three-layer structure. Therefore, we need to prepare $3 \times 2^{3-1}$ types of frequency responses.

C. Models of Broadside-Coupled Lines

Responses of a line segment varies continuously as its length changes. Therefore, instead of a lookup table, appropriate transmission-line models are required. In a multilayer structure, the couplings between lines play an important role. Lines stacked up in a vertical direction especially have significant broadside couplings.

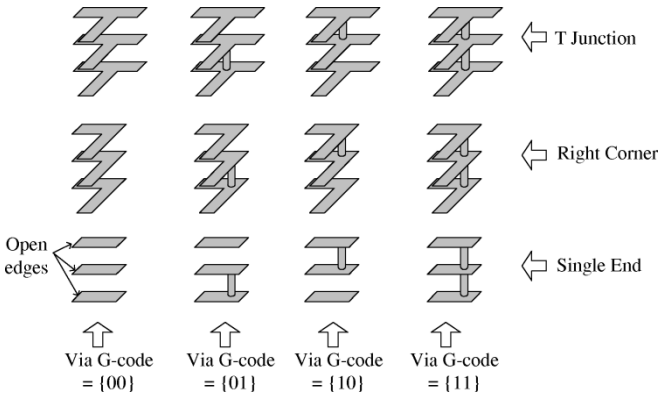

Fig. 2. Three types of discontinuities of intersection points in a P-circuit, and four types of combinations of via connections in a three-layer structure.

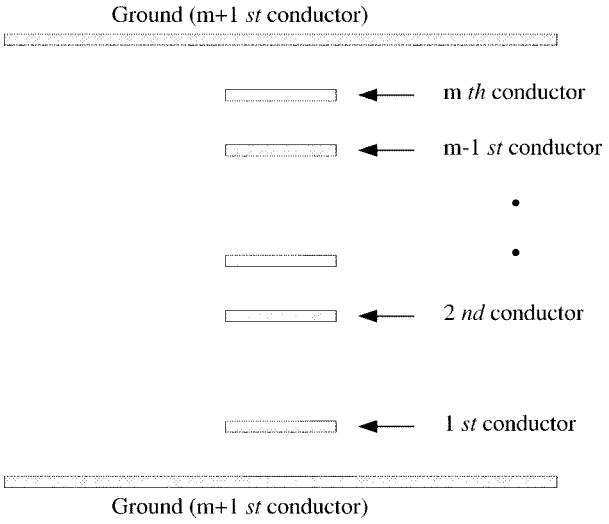

Fig. 3. Cross section of a typical m-conductor transmission line in an N-layer structure.

In this section, we propose a multiconductor transmission-line model with broadside coupling effects in an N-layer structure. Fig. 3 shows a typical multiconductor transmission-line structure in an N-layer. It is not necessary that all N conductors are exist. In this figure, the number of conductors is m, counting from the bottommost one. Both of the top and bottom grounds are numbered as $m+1$. According to a genetic code assigned to each line of a P-circuit, the number of conductors varies from 0 to N, and the number of combinations of such conductors is 2^N.

To obtain characteristic modes of the m-conductor structure, we need to obtain the capacitance C_{ij}, the capacitance between conductor i and conductor j. Note that the number of conductors is $m+1$ if we consider the ground is $m+1$st conductor.

Since $C_{ij} = C_{ji}$ and $C_{ii} = 0$ for $i, j = 1, \ldots, m+1$, the number of unknowns is $((m \times (m+1))/2)$. The values of the unknowns are obtained by the 2-D FEM. If we take notice of the number of combinations picking up two conductors out of $m+1$ conductors also being $((m \times (m+1))/2)$, the efficient computational procedure to obtain all the capacitances would be as follows.

First, the procedure chooses two conductors p and q out of $m+1$ conductors. Let the voltage of the conductors p and q then be 1 V, and let the voltage of the others be zero. Then calculate the energy $E_{\rm system}$ of the system. The capacitance of the system is derived as $C_{\overline{pq}} = 2E_{\rm system}/V^2$ with $V = 1$.

The relation between $C_{\overline{pq}}$ and C_{ij} is

$$C_{\overline{pq}} = \sum_{i,j} C_{ij} - \sum_{i,j\notin\{p,q\}} C_{ij} - C_{pq}. \tag{1}$$

The second term on the right-hand side (RHS) corresponds to the capacitance between conductors of 0 V. The third term corresponds to the capacitance between conductors of 1 V. We introduce a matrix Γ whose elements are

$$\begin{aligned}
&\Gamma_{\overline{pq},ij} = 1, && \text{if } p \in \{i,j\} \text{ but } q \notin \{i,j\}\\
&\Gamma_{\overline{pq},ij} = 1, && \text{if } p \notin \{i,j\} \text{ but } q \in \{i,j\}\\
&\Gamma_{\overline{pq},ij} = 0, && \text{if } p \notin \{i,j\} \text{ and } q \notin \{i,j\}\\
&\Gamma_{\overline{pq},ij} = 0, && \text{if } p \in \{i,j\} \text{ and } q \in \{i,j\}.
\end{aligned} \tag{2}$$

The matrix equation to calculate the elements of the capacitance matrix is then obtained, as shown in (3) at the bottom of this page.

Inversion of the matrix Γ gives the elements of the capacitance matrix

$$\begin{pmatrix} C_{12} \\ C_{13} \\ C_{14} \\ \vdots \\ C_{m,m-1} \\ C_{m,m+1} \end{pmatrix} = \begin{pmatrix} 0 & 1 & 1 & \cdots & 0 & 0 \\ 1 & 0 & 1 & \cdots & 0 & 0 \\ 1 & 1 & 0 & \cdots & 0 & 0 \\ \vdots & \vdots & \vdots & \ddots & \vdots & \vdots \\ 0 & 0 & 0 & \cdots & 0 & 1 \\ 0 & 0 & 0 & \cdots & 1 & 0 \end{pmatrix}^{-1} \begin{pmatrix} C_{\overline{12}} \\ C_{\overline{13}} \\ C_{\overline{14}} \\ \vdots \\ C_{\overline{m,m-1}} \\ C_{\overline{m,m+1}} \end{pmatrix}. \tag{4}$$

The only exception to this technique is the case of $\mathrm{m} = 4$. In this case, $C_{\overline{12}} = C_{\overline{34}}$ and also the field distribution is the same, except that the electric field directs opposite directions. This means the two conditions are physically the same. The case of $C_{\overline{13}}$ and $C_{\overline{24}}$ and the case of $C_{\overline{14}}$ and $C_{\overline{23}}$ are of the same manner. The matrix then becomes singular. In the case of $\mathrm{m} = 4$, the conditions that one of the four conductors is 1 V while the other three are 0 V, as well as the conditions that two conductors are 1 V and the other two are 0 V, can solve the problem.

The characteristic modes of the structure are derived next. The capacitance matrix with the referenced ground conductor is

$$\begin{pmatrix} \sum_{k=1}^{m} C_{1k} & -C_{12} & -C_{13} & -C_{14} & \cdots & -C_{1m} \\ -C_{21} & \sum_{k=1}^{m} C_{2k} & -C_{23} & -C_{24} & \cdots & -C_{2m} \\ -C_{31} & -C_{32} & \sum_{k=1}^{m} C_{3k} & -C_{34} & \cdots & -C_{3m} \\ -C_{41} & -C_{42} & -C_{43} & \sum_{k=1}^{m} C_{4k} & \cdots & -C_{4m} \\ \vdots & \vdots & \vdots & \vdots & \ddots & \vdots \\ -C_{m1} & -C_{m2} & -C_{m3} & -C_{m4} & \cdots & \sum_{k=1}^{m} C_{mk} \end{pmatrix} \tag{5}$$

where the capacitance between conductor i and the ground is redefined as $C_{ii} = C_{i,m+1}$. The characteristic modes correspond to the eigenvectors of the above matrix. We do not mention the way to obtain eigenvectors, but the reader may refer to [11] for additional information.

$$\begin{aligned}
\begin{pmatrix} C_{\overline{12}} \\ C_{\overline{13}} \\ C_{\overline{14}} \\ \vdots \\ C_{\overline{m,m-1}} \\ C_{\overline{m,m+1}} \end{pmatrix} &= \Gamma \begin{pmatrix} C_{12} \\ C_{13} \\ C_{14} \\ \vdots \\ C_{m,m-1} \\ C_{m,m+1} \end{pmatrix} \\
&= \begin{pmatrix} \Gamma_{\overline{12},12} & \Gamma_{\overline{12},13} & \Gamma_{\overline{12},14} & \cdots & \Gamma_{\overline{12},mm-1} & \Gamma_{\overline{12},mm+1} \\ \Gamma_{\overline{13},12} & \Gamma_{\overline{13},13} & \Gamma_{\overline{13},14} & \cdots & \Gamma_{\overline{13},mm-1} & \Gamma_{\overline{13},mm+1} \\ \Gamma_{\overline{14},12} & \Gamma_{\overline{14},13} & \Gamma_{\overline{14},14} & \cdots & \Gamma_{\overline{14},mm-1} & \Gamma_{\overline{14},mm+1} \\ \vdots & \vdots & \vdots & \ddots & \vdots & \vdots \\ \Gamma_{\overline{mm-1},12} & \Gamma_{\overline{mm-1},13} & \Gamma_{\overline{mm-1},14} & \cdots & \Gamma_{\overline{mm-1},mm-1} & \Gamma_{\overline{mm-1},mm+1} \\ \Gamma_{\overline{mm+1},12} & \Gamma_{\overline{mm+1},13} & \Gamma_{\overline{mm+1},14} & \cdots & \Gamma_{\overline{mm+1},mm-1} & \Gamma_{\overline{mm+1},mm+1} \end{pmatrix} \begin{pmatrix} C_{12} \\ C_{13} \\ C_{14} \\ \vdots \\ C_{m,m-1} \\ C_{m,m+1} \end{pmatrix} \\
&= \begin{pmatrix} 0 & 1 & 1 & \cdots & 0 & 0 \\ 1 & 0 & 1 & \cdots & 0 & 0 \\ 1 & 1 & 0 & \cdots & 0 & 0 \\ \vdots & \vdots & \vdots & \ddots & \vdots & \vdots \\ 0 & 0 & 0 & \cdots & 0 & 1 \\ 0 & 0 & 0 & \cdots & 1 & 0 \end{pmatrix} \begin{pmatrix} C_{12} \\ C_{13} \\ C_{14} \\ \vdots \\ C_{m+1,m-1} \\ C_{m+1,m} \end{pmatrix}
\end{aligned} \tag{3}$$

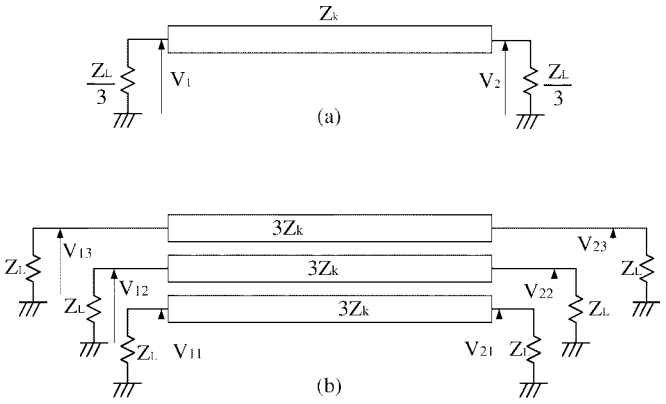

Fig. 4. Two different views of the same m-conductor transmission line terminated by $Z_L\ \Omega$ at all ports as an example of $\mathrm{m} = 3$. (a) The m conductors are considered as one transmission line and terminations are collected into two common terminations at both ends. (b) m conductors with impedance of $m \times Z_k$ are terminated by $Z_L\ \Omega$ at $2m$ terminals.

The characteristic impedance of a certain mode is obtained by the 2-D FEM again. Let $\mathbf{V}_k$ be the kth eigenvector, which corresponds to the kth mode as follows:

$$\mathbf{V}_k = \begin{pmatrix} V_{k1} \\ V_{k2} \\ \vdots \\ V_{km} \end{pmatrix}. \tag{6}$$

The exciting voltages for the first conductor to mth conductor must then be $x_k V_{k1}$ to $x_k V_{km}$, where x_k is a normalizing coefficient of the kth mode to match EM representation with circuit representation. The capacitance C_k of the system excited by the voltages and the capacitance C_{k0} of the same system with the relative permittivity of the material set to one are used to obtain the kth-mode impedance

$$Z_k = \frac{1}{c\sqrt{C_k \times C_{k0}}} \tag{7}$$

where c is the speed of light in free space.

For the case that all $2m$ terminals of m coupled conductors are terminated by $Z_L\ \Omega$, there are two ways of approaching the problem. Fig. 4 is the examples of these two view when $\mathrm{m} = 3$. Fig. 4(a) shows the view that a line with impedance Z_k is terminated by $Z_L/m\ \Omega$ at both ends. This is considered that the m conductors act as one transmission line and terminations are collected into two common terminations at both ends. On the other hand, Fig. 4(b) shows the view of the m conductors with the impedance of $m \times Z_k$ terminated by $Z_L\ \Omega$ at $2m$ terminals. In this view, we assumed all the line impedances of m conductors are the same as $m \times Z_k$. This is true in the case of the eigenmode transmission. If not, the linearity of the voltages at terminals and the currents of lines failed.

The voltage at terminal 2 in Fig. 4(a) is

$$V_2 = \frac{\dfrac{Z_L}{m}}{\dfrac{Z_L}{m}\cos\beta l + jZ_k \sin\beta l} V_1 \equiv ZV_1 \tag{8}$$

and at terminal $2i$ in Fig. 4(b) is

$$V_{2i} = \frac{Z_L}{Z_L \cos\beta l + jmZ_k \sin\beta l} V_{1i} = ZV_{1i} = Zx_k V_{ki}. \tag{9}$$

The power consumption at the load is

$$P_L = \frac{1}{2}\frac{V_2^2}{\dfrac{Z_L}{m}} \tag{10}$$

in Fig. 4(a) and

$$P_L' = \frac{1}{2}\sum_i^m \frac{V_{2i}^2}{Z_L} \tag{11}$$

in Fig. 4(b). The equation to determine x_k is then

$$P_L = P_L' \tag{12}$$

or

$$mV_1^2 = \sum_i^m x_k^2 V_{ki}^2. \tag{13}$$

What we need to obtain is the value of x_k when $V_1 = 1$ so as to match the definition of the impedance of EM representation, which are determined by E_{system}, and that of circuit representation

$$x_k = \sqrt{\frac{m}{\sum_i^m V_{ki}^2}}. \tag{14}$$

Once all the mode impedances are obtained, the S-parameters of the m-conductor transmission line can be derived via a conventional way [12]. Fig. 5 shows an explanatory diagram of superposing reflection coefficients of modes with short or open conditions at the middle points of the lines. Properly chosen coefficients realize a condition of one-port excitation. To excite port j by 1 V and the other ports by 0 V, the mode i must be excited a_{ij} times of $x_k \mathbf{V}_i$, which is the eigenvector corresponding to the mode i. This condition can be expressed as

$$(x_1\mathbf{V}_1, x_2\mathbf{V}_2, \cdots\cdots, x_{m-1}\mathbf{V}_{m-1}, x_m\mathbf{V}_m) \begin{pmatrix} a_{1j} \\ a_{2j} \\ \vdots \\ \vdots \\ a_{m-1,j} \\ a_{m,j} \end{pmatrix} = \begin{pmatrix} 0 \\ \vdots \\ 1 \\ 0 \\ \vdots \\ 0 \end{pmatrix} \begin{matrix} \\ \\ \leftarrow 1 \\ \leftarrow j \\ \\ \leftarrow m \end{matrix}. \tag{15}$$

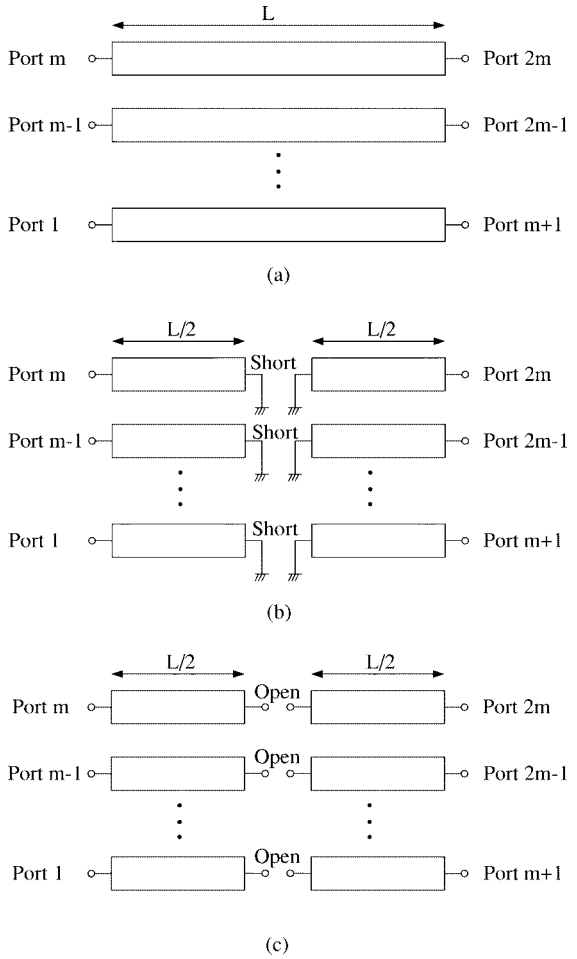

Fig. 5. Diagram to explain derivation of the scattering parameters. The scattering parameters are obtained by superposing reflection coefficients of modes with short or open boundary conditions at the middle point of the lines. (a) The m-conductor transmission line. (b) The reflection with short conditions at middle points. (c) The reflection with open conditions at middle points.

The exciting coefficients a_{ij} will be

$$\begin{pmatrix} a_{1j} \\ a_{2j} \\ \vdots \\ \vdots \\ a_{m-1,j} \\ a_{m,j} \end{pmatrix} = (x_1\mathbf{V}_1, x_2\mathbf{V}_2, \cdots\cdots, x_{m-1}\mathbf{V}_{m-1}, x_m\mathbf{V}_m)^{-1} \times \begin{pmatrix} 0 \\ \vdots \\ 1 \\ 0 \\ \vdots \\ 0 \end{pmatrix}. \quad (16)$$

Let the reflection coefficient for excitation of mode k with an open condition at the middle point of the line be Γ_{ko}, and with a short condition be Γ_{ks} as follows:

$$\Gamma_{ko} = \frac{Z_{ko} - Z_L}{Z_{ko} + Z_L}$$
$$Z_{ko} = -jmZ_k \cot\left(\frac{\beta l}{2}\right) \quad (17)$$

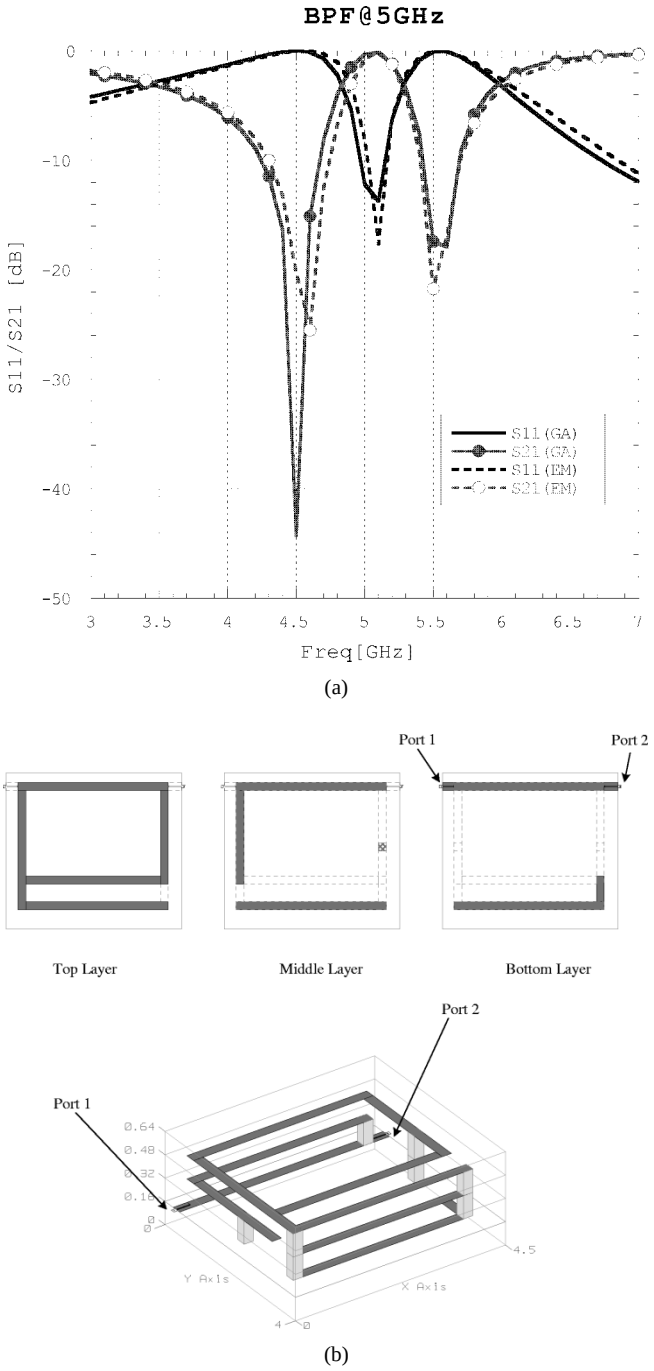

Fig. 6. Bandpass filter whose passband is from 4.9 to 5.1 GHz, and stopbands are from 4.4 to 4.5 and 5.5 to 5.6 GHz. (a) Circuit patterns in a three-layer structure. (b) Responses of the GA design and EM simulation of the bandpass filter.

$$\Gamma_{ks} = \frac{Z_{ks} - Z_L}{Z_{ks} + Z_L}$$
$$Z_{ks} = jmZ_k \tan\left(\frac{\beta l}{2}\right). \quad (18)$$

The excited voltage at port i is then

$$V_i = \frac{1}{2}\left(\sum_k^m a_{kj}x_kV_{ki}\Gamma_{ko} + \sum_k^m a_{kj}x_kV_{ki}\Gamma_{ks}\right) = S_{ij} \quad (19)$$

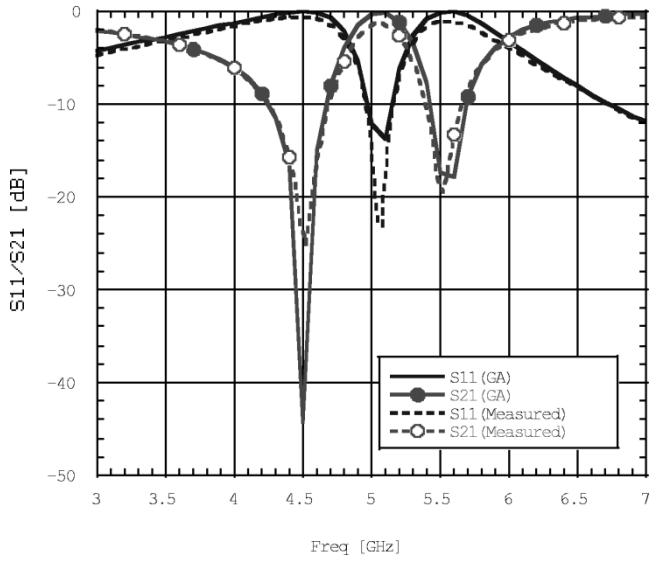

(c)

Fig. 6. *(Continued.)* Bandpass filter whose passband is from 4.9 to 5.1 GHz, and stopbands are from 4.4 to 4.5 and 5.5 to 5.6 GHz. (c) Responses of the GA design and the measurement of the bandpass filter

for the exciting side and

$$V_{i+m}=\frac{1}{2}\left(\sum_{k}^{m}a_{kj}x_kV_{ki}\Gamma_{ko}-\sum_{k}^{m}a_{kj}x_kV_{ki}\Gamma_{ks}\right)=S_{i+m,j}. \tag{20}$$

for the far side. The complete S-parameters are found by repeating the equations from (15)to (20) with j from 1 to m.

The obtained S-parameters of multiconductor transmission lines are connected to the S-parameters of vias obtained in the previous section. The response of the whole structure is calculated much faster than full-wave EM simulations.

IV. Design Examples of Microwave Circuits

In this section, two kinds of microwave circuits are design and verified. The material is supposed to be low-temperature co-fired ceramics (LTCCs), which would be the major material for multichip modules (MCMs) in mobile terminal equipments these days. The circuits have a three-layer structure with a relative permittivity of 7.1 whose wave length at 5 GHz is 22.5 mm. Each layer has a thickness of 160 μm and a linewidth of 200 μm. The assigned maximum circuit size was 5×5 mm^2.

A. Bandpass Filters

The first design example is a bandpass filter. Its passband is 4.9–5.1 GHz with an insertion loss less than 0.5 dB, and stopbands are from 4.4 to 4.5 and 5.5 to 5.6 GHz with a rejection over 15 dB. Fig. 6(a) shows the obtained circuit, and Fig. 6(b) shows the comparison between the GA model (solid lines) and EM simulation[1] (dashed lines) and Fig. 6(c) shows the comparison between the GA model (solid lines) and measured results (dashed lines). The obtained size of the outermost pattern was 3.67 mm $\times$ 3.05 mm. Once the GA proposes the circuit pattern, neither further modifications, nor precise simulations are required. The computation time of the EM simulation was approximately 30 s per one frequency on a Pentium III 700-MHz personal computer (PC). The computation time of the GA process was approximately 40 h on the same PC, with 200 circuits tested at eight frequencies through 200 generations. These results agree well, except for the insertion loss due to our using a lossless line model in the GA. The maximum loss in the passband was 2.48 dB at 4.9 GHz.

[1]EM sight with *AWR Microwave Office 2001,* ver.4.01.

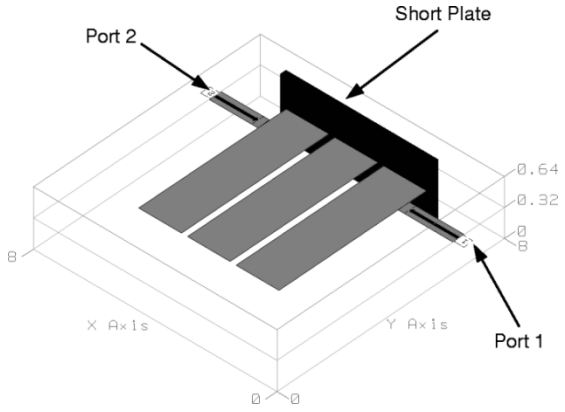

(a)

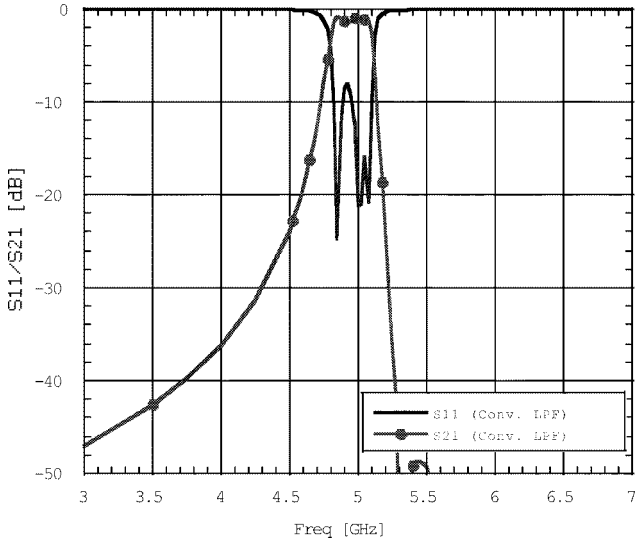

(b)

Fig. 7. (a) Conventional three-quarter-wavelength-resonator bandpass filter. (b) Responses of the roughly designed conventional filter.

Conventional design requires two or three resonators whose lengths are about a quarter-wavelength. Fig. 7(a) shows a design example of a conventional three-resonator bandpass filter. Fig. 7(b) shows the result of EM simulation of the conventional filter, which needs further optimization to improve the reflection. The shorted resonator length was 5.4 mm, and the width was 1.4 mm. The total size was 5.4 mm $\times$ 4.6 mm. The size of the GA-produced filter was slightly small, but not significant. However, if more than one passband was required, the conventional procedure encountered difficulty, while the GA design had no such restriction.

The second bandpass filter has a passband at 4.9–5.1 GHz with the insertion loss less than 0.25 dB, and stopbands are

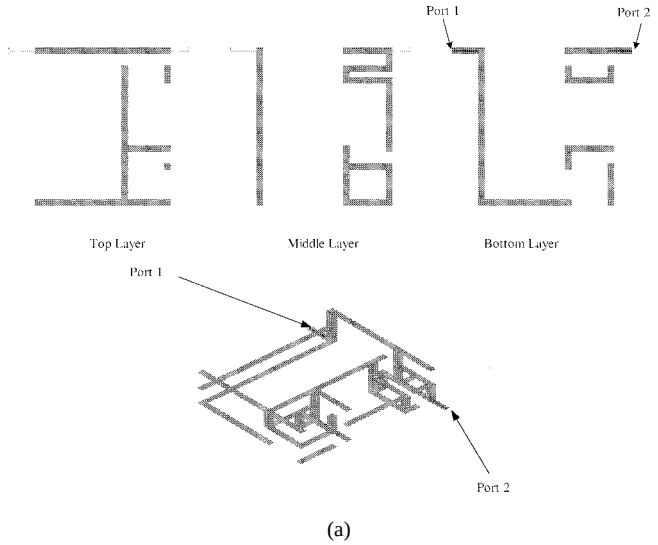

(a)

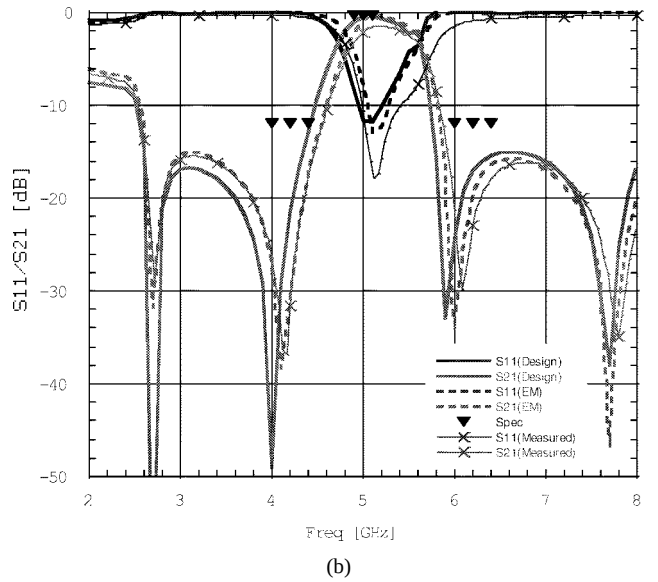

(b)

Fig. 8. Bandpass filter whose passband is from 4.9 to 5.1 GHz and stopbands are from 4.0 to 4.4 and 6.0 to 6.4 GHz. (a) Circuit patterns in three-layer structure. (b) Responses of the GA design, EM simulation, and measurement of the second bandpass filter.

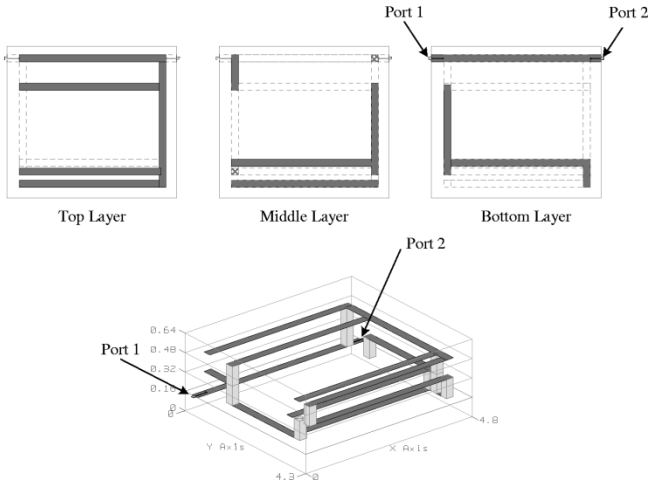

(a)

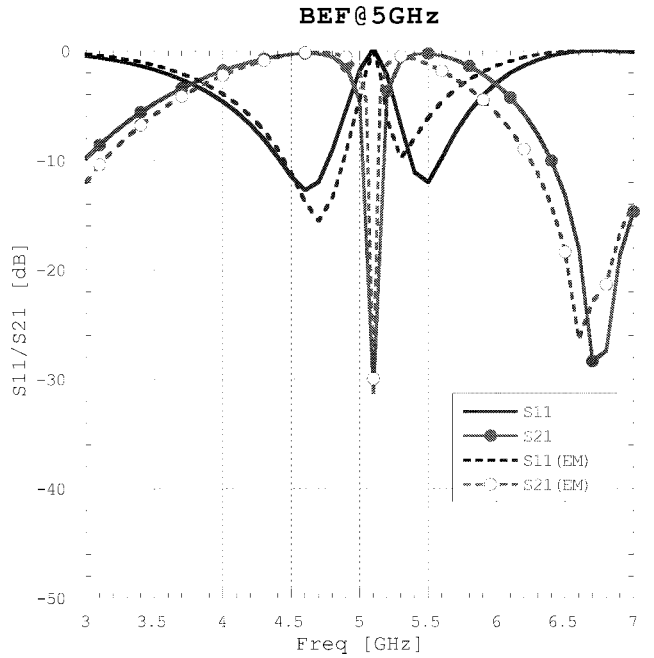

(b)

Fig. 9. Bandstop filter whose stopband is from 5.0 to 5.1 GHz, and passbands are from 4.6 to 4.8 and 5.3 to 5.5 GHz. (a) Circuit patterns in a three-layer structure. (b) Responses of the bandpass filter.

from 4.0 to 4.4 and 6.0 to 6.4 GHz with a rejection over 12 dB. Fig. 8(a) shows the obtained circuit and Fig. 8(b) shows the comparison between the GA model (solid lines) and EM simulation (dashed lines) and measured results (thin solid lines with markers). The obtained size of the outermost pattern was 4.15 mm × 4.85 mm. The computation time of the GA process was approximately 9 h on the same PC, with 300 circuits tested at nine frequencies through 54 generations. These results agree well, except for the insertion loss. The maximum loss in the passband was 2.9 dB at 4.9 GHz.

B. Bandstop Filter

The third design example is a bandstop filter. Its stopband is 5.0–5.1 GHz with the rejection over 12 dB, and passbands are from 4.6 to 4.8 and 5.3 to 5.5 GHz with the insertion loss less than 0.7 dB. Fig. 9(a) shows the obtained circuit, and Fig. 9(b) shows the comparison between the GA model (solid lines) and EM simulation (dashed lines). The size of the outermost pattern was 3.93 mm × 3.57 mm. The computation time of the EM simulation of the circuit was approximately 40 s per one frequency on a Pentium III 700-MHz PC. The computation time of the GA process was approximately 20 h on the same PC, with 200 circuits tested at eight frequencies through 100 generations. The EM simulation showed a narrower bandwidth of the stopband than the GA result. This was due to the coupling effects that the GA did not considered. Those might be the couplings between lines not overlapped and the couplings between vias. Though the pattern contained closely disposed five lines in three layers, only the two pair of the lines were considered as coupled lines that overlapped in the different layers. This example were not fabricated.

V. Discussions and Conclusions

We have introduced an evolutionary generation of 3-D microwave line-segment circuits embedded in a multilayer structure. The developed procedure optimizes a line-segment circuit with a variety of topology, and ends up with a circuit that exceeds expectations. Our developing multiconductor transmission-line model enables computation time to be practical.

To make the GA converge well, arbitrary sets of parameters in our process correspond with certain feasible circuits without any lines crossing or without disconnecting each other in physical space. This is very important to avoid convergence to meaningless solutions.

Performing several design examples, we can say that our procedure proposes good solutions in practical time for specifications with narrow stopbands and/or narrow passbands compared to ones with wide passbands. This is because the process is prone to create the complex structure that usually has sharp frequency characteristics. For a design with widely uniform frequency characteristics, some restrictions to make circuits simple should be introduced, such as a reduction of the number of lines or restrictions of a circuit's size.

Insertion-loss estimation is another shortcoming of this procedure. An accurate estimation of this characteristic is difficult because the loss of each mode cannot simply be summed up to obtain the total loss. Some margins should be taken into account and specifications with reflection loss seem to offer a good convergence instead of the ones with insertion loss.

Couplings between lines that are disposed closely to each other, but are not overlapped might be taken into account for a more accurate design. In this paper, keeping a certain minimum interval between such lines reduces the unexpected coupling effect. However, in the example of the bandstop filter, such couplings still caused a discrepancy in the calculation. In a thick layer structure, couplings between vias should also be considered. These coupling considerations are tradeoffs between compactness of the circuit and reduction of computation time or complexity of the procedure.

Notwithstanding, performed examples verified the validity of combination of the GA optimization and the proposed broadside-coupled transmission-line model for compact 3-D microwave line-segment circuit designs. The result showed the model were good enough to design microwave circuits without EM simulation, except for the circuit including closely disposed, but not overlapped lines.

If the conventional techniques were used, starting from a prototype ladder circuit, the procedure would propose a certain size of resonators. To minimize the size less than a quarter-wavelength, the resonators must be bent in the multilayer structure by trial-and-error EM simulation, or if the lumped-element components are used for lower frequency specifications, inductors must be designed by EM simulations, and a certain accurate model that can express parasitic capacitances to other components must be required. Even in this case, there is no guarantee that the circuit is realized with the desired size. In the case of a bandpass filter with more than one passband, the conventional procedure requires several stopbands to be superposed on a wide passband. For the case that such passbands are disposed far apart, in other words, the superposed passband is pretty wide, the conventional procedure becomes difficult to perform.

Our proposed GA process searches for solutions not only in ladder circuits, but also in a wide variety of possible topology realized in the structure. Some topologies utilize phase interference effects to make stopbands. Others create resonators with several resonant frequencies. Analysis of the obtained circuits has a chance to propose new types of filter circuits.

Since no initial value is required and what we need to do is simply input specifications, designing circuit topology and dimensions by the GA will be one of the strong methods in future CAD technologies.

Acknowledgment

The authors would like to thank Prof. N. G. Alexopoulos, University of California at Irvine, for useful discussions, guidance, and advice. The authors are also grateful to Prof. F. De Flaviis, University of California at Irvine, for technical suggestions.

References

[1] T. Nishino and T. Itoh, "Evolutionary generation of microwave line-segments circuits by genetic algorithms," *IEEE Trans. Microwave Theory Tech.*, vol. 50, pp. 2048–2055, Sept. 2002.

[2] J. H. Holland, *Adaptation in Natural and Artificial Systems*. Ann Arbor, MI: Univ. Michigan Press, 1975.

[3] E. Michielssen, J. M. Sajer, and R. Mittra, "Design of multilayered FSS and wave guide filter using genetic algorithms," in *IEEE AP-S Int. Symp. Dig.*, 1993, pp. 1936–1939.

[4] J. M. Johnson and Y. Rahmat-Samii, "Genetic algorithms and method of moments (GA/MoM): A novel integration for antenna design," in *IEEE AP-S Int. Symp. Dig.*, 1997, pp. 1664–1667.

[5] J. R. Koza, F. H. Bennett, D. Andre, M. A. Keane, and F. Dunlap, "Automated synthesis of analog electrical circuits by mean of genetic programming," *IEEE Trans. Evol. Comput.*, vol. 1, pp. 109–128, Apr. 1997.

[6] A. John and R. H. Jansen, "Evolutionary generation of (M)MIC component shapes using 2.5D EM simulation and discrete genetic optimization," in *IEEE MTT-S Int. Microwave Symp. Dig.*, 1996, pp. 745–748.

[7] D. Pavlidis and H. L. Hartnagel, "The design and performance of three-line microstrip couplers," *IEEE Trans. Microwave Theory Tech.*, vol. MTT-24, pp. 631–640, Oct. 1976.

[8] S. Yamamoto, T. Azakami, and K. Itakura, "Coupled strip transmission line with three center conductors," *IEEE Trans. Microwave Theory Tech.*, vol. MTT-14, pp. 446–461, Oct. 1966.

[9] C. R. Paul, *Analysis of Multiconductor Transmission Lines*. New York: Wiley, 1994.

[10] N. Fache, F. Olyslager, and D. De Zutter, *Electromagnetic and Circuit Modeling of Multiconductor Transmission Lines*. Oxford, U.K.: Oxford Sci., 1992.

[11] W. H. Press, S. A. Teukolsky, W. T. Vetterling, and B. P. Flannery, *Numerical Recipes in Fortran*, 2nd ed. Cambridge, U.K.: Cambridge Univ. Press, 1992, ch. 11.

[12] R. E. Collin, *Foundations for Microwave Engineering*, 2nd ed. New York: Mc-Graw Hill, 1992, pp. 427–432.

Tamotsu Nishino (M'92) received the B.E. and M.E. degrees in electrical engineering from Waseda University, Tokyo, Japan, in 1989 and 1991, respectively, and the Ph.D. degree in electrical engineering from the University of California at Los Angeles (UCLA), in 2002.

In 1991, he joined the Mitsubishi Electric Corporation, Kanagawa, Japan, where he has been engaged in research and development of antenna feeds systems, microwave amplifiers, microwave control circuits, and microwave module integration. From 1996 to 1997, he was a Visiting Scholar with UCLA.

Tatsuo Itoh (S'69–M'69–SM'74–F'82) received the Ph.D. degree in electrical engineering from the University of Illinois at Urbana-Champaign, in 1969.

From September 1966 to April 1976, he was with the Electrical Engineering Department, University of Illinois at Urbana-Champaign. From April 1976 to August 1977, he was a Senior Research Engineer with the Radio Physics Laboratory, SRI International, Menlo Park, CA. From August 1977 to June 1978, he was an Associate Professor with the University of Kentucky, Lexington. In July 1978, he joined the faculty at The University of Texas at Austin, where he became a Professor of Electrical Engineering in 1981 and Director of the Electrical Engineering Research Laboratory in 1984. During the summer of 1979, he was a Guest Researcher with AEG-Telefunken, Ulm, Germany. In September 1983, he was selected to hold the Hayden Head Centennial Professorship of Engineering at The University of Texas at Austin. In September 1984, he was appointed Associate Chairman for Research and Planning of the Electrical and Computer Engineering Department, The University of Texas at Austin. In January 1991, he joined the University of California at Los Angeles (UCLA) as Professor of Electrical Engineering and Holder of the TRW Endowed Chair in Microwave and Millimeter Wave Electronics. He was an Honorary Visiting Professor with the Nanjing Institute of Technology, Nanjing, China, and at the Japan Defense Academy. In April 1994, he was appointed an Adjunct Research Officer with the Communications Research Laboratory, Ministry of Post and Telecommunication, Japan. He currently holds a Visiting Professorship with The University of Leeds, Leeds, U.K. He has authored or coauthored 310 journal publications, 640 refereed conference presentations, and has written 30 books/book chapters in the area of microwaves, millimeter waves, antennas, and numerical electromagnetics. He has generated 60 Ph.D. students.

Dr. Itoh is a member of the Institute of Electronics and Communication Engineers of Japan, and Commissions B and D of USNC/URSI. He served as the editor of the IEEE TRANSACTIONS ON MICROWAVE THEORY AND TECHNIQUES (1983–1985). He serves on the Administrative Committee of the IEEE Microwave Theory and Techniques Society (IEEE MTT-S). He was vice president of the IEEE MTT-S in 1989 and president in 1990. He was the editor-in-chief of IEEE MICROWAVE AND GUIDED WAVE LETTERS (1991–1994). He was elected an Honorary Life Member of the IEEE MTT-S in 1994. He was elected a member of the National Academy of Engineering in 2003. He was the chairman of the USNC/URSI Commission D (1988–1990) and chairman of Commission D of the International URSI (1993–1996). He is chair of the Long Range Planning Committee of the URSI. He serves on advisory boards and committees of a number of organizations. He has been the recipient of numerous awards including the 1998 Shida Award presented by the Japanese Ministry of Post and Telecommunications, the 1998 Japan Microwave Prize, the 2000 IEEE Third Millennium Medal, and the 2000 IEEE MTT-S Distinguished Educator Award.